Tellus SERIES B CHEMICAL AND PHYSICAL METEOROLOGY
PUBLISHED BY THE INTERNATIONAL METEOROLOGICAL INSTITUTE IN STOCKHOLM

Tellus (2010), 62B, 160–171
Printed in Singapore. All rights reserved

TELLUS

The vertical distribution of atmospheric DMS in the high Arctic summer

By JENNY LUNDÉN[1]*, GUNILLA SVENSSON[1], ARMIN WISTHALER[2], MICHAEL TJERNSTRÖM[1], ARMIN HANSEL[2] and CAROLINE LECK[1], [1]*Department of Meteorology Stockholm University, 106 91 Stockholm, Sweden*; [2]*Institut für Ionenphysik and Angewandte Physik, Universität Innsbruck, Innsbruck, Austria*

(Manuscript received 27 January 2010; in final form 8 April 2010)

ABSTRACT

The vertical structure of gas-phase dimethyl sulphide [DMS(g)] in the high Arctic atmosphere is investigated during a summer season. The model results show that the near-surface DMS(g) concentration over open ocean is very variable both in time and space, depending on the local atmospheric conditions. Profiles over ocean have typically highest concentration near the surface and decrease exponentially with height. Over the pack-ice, the concentrations are typically lower and the vertical structure changes as the air is advected northward. Modelled DMS(g) maxima above the local boundary layer were present in about 3% of the profiles found over the pack-ice. These maxima were found in association to frontal zones. Our results also show that DMS(g) can be mixed downward by turbulence into the local boundary layer and act as a local near-surface DMS(g) source over the pack-ice and may hence influence the growth of cloud condensation nuclei and cloud formation in the boundary layer. Profile observations are presented in support to the model results. They show that significant DMS(g) concentrations exist in the Arctic atmosphere at altitudes not to be expected when only considering vertical mixing in the boundary layer.

1. Introduction

The existence of clouds and their impact on the energy balance at the surface is of high importance for the Arctic climate. Clouds modify the incoming short-wave radiation and confine the outgoing long-wave radiation. Especially low-level clouds are common in the Arctic atmosphere and over the pack-ice they tend to have a warming effect for most of the annual cycle, in contrast to low marine stratiform clouds at lower latitudes (Intrieri et al., 2002). Arctic clouds are not well represented in models and their radiative impact on the surface energy balance is not correctly captured (Curry, 1995; Wyser et al., 2008; Karlsson and Svensson, 2010). Clear, cloud free, conditions are rare in the models and occur more seldom than in the real atmosphere (Tjernström et al., 2008). When clouds are present, there is large spread in their microphysical properties (e.g. Klein et al., 2009; Karlsson and Svensson, 2010) that in turn depend on the properties of the cloud condensation nuclei (CCN). The presence of low-level clouds during the high Arctic summer results in efficient scavenging and as a result CCN are scarce (Heintzenberg and Leck, 1994; Bigg et al., 1996; Lohmann and Leck, 2005). The process of forming new low-level clouds is dependent on the presence of CCN near the surface. Leck and Bigg (2007) argued that CCN number concentration is not determined by the oxidation products of dimethyl sulphide (DMS), as has usually been assumed (Charlson et al., 1987), but by the concentration in the air of biogenic particulate matter derived from the ocean surface by bubble bursting. The production of DMS by phytoplankton would still be involved. The concentration of DMS oxidation products determine the growth of pre-existing particles in the atmosphere which influence their cloud nucleation properties.

During the Arctic summer, from June to August, the melting pack-ice, with its leads and melt ponds, influence the local climate. The ice regulates the temperature at the surface; additional energy input melts the ice rather than warming the surface whereas energy loss refreezes the water instead of cooling the surface. Thus, the near-surface temperature is often ranging between 0 and $-2\,^{\circ}$C, the melting point of snow and ice and the freezing point of salt ocean water. Due to the presence of ice the near-surface humidity is close to saturation. The large-scale advection of warmer air from south creates an overall stably stratified atmosphere with a shallow frequently near-neutral about 200 m deep boundary layer capped by an inversion (Tjernström,

*Corresponding author.
e-mail: jenny.lunden@gmail.com
DOI: 10.1111/j.1600-0889.2010.00458.x

2005). This structure limits the vertical exchange between the boundary layer and the free atmosphere.

The melting ice in the marginal ice zone is favourable for the production of dimethylsulfoniopropionate and aqueous phase dimethyl sulphide [DMS(aq)] which is released by phytoplankton (Leck and Persson, 1996a; Matrai and Vernet, 1997). In the Arctic (north of 70°N) the concentration is over all high and DMS(aq) show a seasonal variability due to its biological origin (Bates et al., 1987; Leck and Persson, 1996a). After the summer peak, DMS(aq) is shown to follow an exponential decay, decreasing about three orders of magnitude in concentration between August and October (Leck and Persson, 1996a).

DMS(aq) is transported to the atmosphere via diffusion and turbulence where it is photo-chemically oxidized and produce a variety of sulphur containing compounds, as e.g. methane sulphonic acid, sulphur dioxide and sulphuric acid (Leck and Persson, 1996b). Sulphur constituents can through heterogenic condensation aid growth of pre-existing particles to become large enough to act as CCN and thereby contribute to cloud formation (Leck et al., 2004; Leck and Bigg, 2005; Lohmann and Leck, 2005). This is particularly important in remote areas such as the Arctic, especially in the summer when the anthropogenic influence is limited.

Observations of DMS in the Arctic are sparse relative to observations at lower latitudes. In the Arctic, observations of DMS have mainly been collected during field campaigns at separate locations and along transects from the ocean into the pack-ice (Staubes and Georgii, 1993; Levasseur et al., 1994; Ferek et al., 1995; Leck and Persson, 1996a,b; Matrai and Vernet, 1997; Sharma et al., 1999; Bouillon et al., 2002). Exceptionally little information is found about the vertical structure of atmospheric DMS.

Observational studies have previously shown rapid changes in near-surface DMS(g) concentration (Leck et al., 1996; Bigg et al., 1996, 2001) in the high Arctic. These changes occurred on timescales from minutes to hours, with a magnitude sometimes exceeding the entire seasonal variability. Bigg et al. (1996) hypothesized that they resulted from stratification in DMS(g) concentration with altitude, combined with episodes of mixing from a higher level to the usually very shallow surface mixed layer in which the measurements where made. Suggested explanations for these rapid changes include different processes in the atmosphere, such as transport and mixing in the boundary layer, location of sources, change of air mass and the vertical structure of the atmosphere. The nature of the mixing events was deduced from the wide range of possibilities simply by their effects on DMS(g) and as far as possible on the sparse meteorological records. However, it remained only deduction -no evidence was available either that there where strong concentration gradients or that mixing between the surface mixed layer and overlaying layers occurred.

In order to gain further insights in both the vertical distribution of DMS(g) over the pack-ice area and the possibility of mixing from a higher level to the surface level were measurements were usually made, this study investigated the vertical distribution of DMS(g) in a two month long regional model simulation covering July and August 2001.

The atmospheric part of the Coupled Ocean/Atmospheric Mesoscale Prediction System (COAMPS®) is used with DMS(g) treated as a tracer. The flux of DMS at the sea surface is calculated using a prescribed ocean concentration (see Section 2.2). The same model was successfully used, with a similar setup, to simulate a 10-d period. In that study, the model results are evaluated using observations of DMS(g) in over the pack-ice (Lundén et al., 2007).

This paper is arranged in the following way. In Section 2, the model and model setup are presented. The vertical distribution of DMS(g) concentration over ocean is presented in Section 3.1, starting with the time evolution of DMS(g) vertical profiles from one grid point followed by a general view of DMS(g) concentrations over the open ocean. Then the vertical distribution of DMS(g) over the pack-ice presented starting with a general view in Section 3.2, a statistical analysis of DMS(g) vertical profiles (Section 3.3). This is followed by a Section on observations (Section 3.4) and a case study is discussed in Section 3.5. Finally, some concluding remarks are presented in Section 4.

2. Method

2.1. Model description

COAMPS® is a numerical weather forecast model developed by the US Navy (Hodur, 1997). The atmospheric part of COAMPS® version 3.1 is used in this study in which a system of non-hydrostatic equations for momentum, potential temperature and moisture is solved. The model has previously been evaluated for simulating Arctic conditions (e.g. Tjernström et al., 2005; Rinke et al., 2006; Wyser et al., 2008; Birch et al. 2009). The model has different parametrization for processes that are not resolved on the model grid, e.g. small-scale processes in the boundary layer, precipitation and radiation (Hodur, 1997). The model also has an advanced tracer module where transport and mixing of the tracer is calculated. More information about COAMPS® is found at http://www.nrlmry.navy.mil/coamps-web/web/home.

When diagnosing the boundary layer height in the model, the turbulence in boundary-layer clouds are taken into account. If low-level clouds are present, the boundary layer height is taken where two consecutive grid points have a lapse rate of liquid water potential temperature greater than a critical lapse rate of 3.0×10^{-3} K m^{-1} and that turbulent kinetic energy have dropped to less than 20% of the maximum value at the levels below. Otherwise, the top of the boundary layer is based on the Richardson's number (Ri); the lowest altitude at which Ri exceeds a critical value of 0.5 is taken as the top of the boundary

layer. A minimum of 50 m depth is used for the diagnosed boundary layer depth.

2.2. Modelling DMS

DMS is exchanged at the ocean surface, a process which is highly influenced by the atmospheric turbulence. The water concentration of DMS is supersaturated relative to the air in most areas, thus, the net flux is to the atmosphere. Emitted DMS is transported with horizontal and vertical winds as well as mixed vertically by turbulence. Once in the atmosphere, DMS(g) undergoes photo-chemical oxidation.

In the model simulation DMS(aq) concentration is described by an exponential function based on observations from the Global Surface Seawater Database (http://saga.pmel.noaa.gov/dms, Kettle et al., 1999). The data utilized for the function were collected in the Atlantic sector of the Arctic Ocean (70°N–90°N, 40°W–90°E) during a summer season (June–August) spread over ten years from 1987 to 2007. Data collected around Iceland were also included. The calculated seasonal decline used in the model is 21% per week between July and August. The same seasonal function is used for all open ocean grid points where the DMS flux is calculated using the formulation by Liss and Merlivat (1986).

Detailed chemical aspects of DMS(g) are not considered in the model, the assumption is that the photo-chemical oxidation of DMS(g) can be described by an exponential decay. A decay rate of 1.79 d was used, i.e. after 3 d of advection only 20% of the original DMS(g) is left. The decay rate was estimated with a box model calculation representative for 2001; the Regional Atmospheric Chemistry Mechanism, (RACM, Stockwell et al., 1997) with a DMS scheme from Capaldo and Pandis (1997) and updated rate coefficients for initial reactions of DMS(g), hydroxyl (OH) and nitrate (NO_3, Atkinson et al., 2004).

The first 16 d of the 78 d long simulation, starting on 15 June 2001, are regarded as spin-up time for DMS(g), to establish the concentration over the pack-ice, and are thus not considered in the analysis. Over the pack-ice, the contribution from local DMS(g) sources such as leads and melt ponds is minor compared to DMS(g) advected from the oceans (Leck and Persson, 1996a). Due to the rather coarse resolution of the model grid (50 km × 50 km), small-scale features in the ice were not resolved. Thus contributions from leads and melt ponds in the pack-ice are not taken into account; all modelled DMS(g) over the pack-ice is advected from the surrounding oceans. A more detailed description of the flux calculation is found in Lundén et al. (2007) where an evaluation of the modelled DMS(g) with observations from the Arctic also is presented. The main conclusion from Lundén et al. (2007) is that the time development of observed DMS(g) is captured by the model with a correlation coefficient 0.76.

2.3. Model setup

Figure 1 shows the area of study, covering the Arctic region (north of 70°N) including the entire pack-ice area as well as the source regions for DMS in the adjacent seas. The model grid contained 111 × 111 grid points with a horizontal resolution

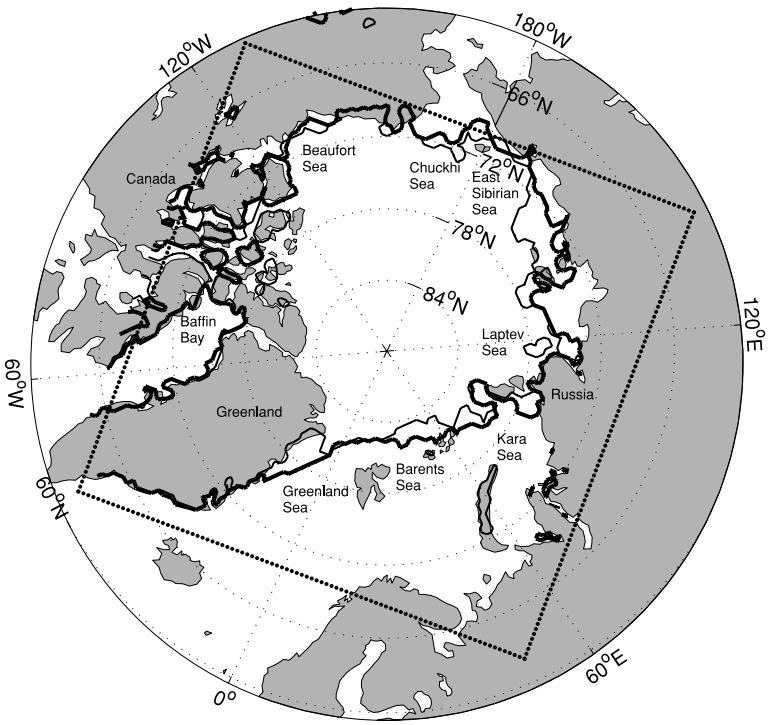

Fig. 1. The model grid with the average ice cover in July (thick line) and in August (thin line), 2001.

of 50 km × 50 km and 46 vertical levels, the lowest at 3 m and the highest at 31 km. To resolve processes in the boundary layer, the vertical levels followed an exponential increase with one third of the levels situated below 500 m. Re-analysis fields from the European Centre for Medium-Range Weather Forecasts (ECMWF) with spatial resolution of 1° × 1° were used for initialization and for updating the boundary conditions with 6 hr intervals. For the lower boundary, sea surface temperature and ice fraction were derived from satellite observations using Advanced Very High Resolution Radiometer (AVHRR) and Special Sensor Microwave Imager (SSMI), respectively. The ice cover in the model was updated every 24 h. The ice surface temperature is calculated with a thermodynamic ice model with separate energy balance for snow and ice. The model have a fixed ice thickness with a deep layer temperature set by the freezing point of salty water (−1.8 °C). A simplified snow model is applied at the surface where the snow layer is allowed to melt and refreeze and the modelled snow albedo change when new snow fall on the surface (Birch et al., 2009).

3. Results and discussion

3.1. Vertical DMS(g) distribution over ocean

Figure 2a shows the time-height cross-section of near-surface DMS(g) concentration from a grid column over Barents Sea (77°N, 44°E) for the two simulated months. The DMS(g) concentration shows a large temporal variability, between 1 and 32 nmol m^{-3} at this location. The flux of DMS(g), and hence the near-surface concentration, is determined by DMS(aq) concentration at the air–sea interface and the efficiency of the transfer velocity that is dependent on the local wind speed (see Fig. 2a). The vertical turbulent mixing in the atmospheric boundary layer determines the height to which the DMS(g) concentration is well mixed. Higher boundary layer concentrations in a deep boundary layer are found when the wind speed is stronger giving rise to both a higher surface exchange and stronger turbulent mixing (see Fig. 2a). The lower concentrations may be associated with lower wind speeds at the surface or stronger vertical mixing caused by, for example, clouds since they are usually turbulent.

The typical vertical DMS(g) distribution is shown in Fig. 2b where the median profile for all ocean grid points between 70°N and 80°N is presented. The presence of a source is clearly visible in the figure as the concentration is highest close to the surface, 5 and 16 nmol m^{-3} for the median and 95th percentiles, respectively. The DMS(g) concentration declines exponentially with altitude and is close to zero at approximately 700 m (2 km for the 95th percentile). The relatively high concentrations, up to 2 nmol m^{-3}, occasionally found at 1 km height above sea level (a.s.l.) are due to events with strong vertical mixing. It is clear from this analysis that the variability in the DMS(g) concentrations over the open ocean is large. Depending on time and location the air that is advected in over the pack-ice contains more or less DMS(g). However, the vertical structure of the DMS(g) concentration over ocean is similar, with highest concentration near the surface and an exponentially decrease above. The situation is quite different over the pack-ice region as will be discussed in the following sections.

3.2. Vertical DMS(g) distribution over ice

To investigate the occurrence of DMS(g) concentration the pack-ice area was divided into four, 5° wide, latitude bands from 70°N to 90°N. Figure 3 shows median and 95th percentile DMS(g) concentration profiles over ice reaching from 3 m (the lowest level in the model) up to 5 km.

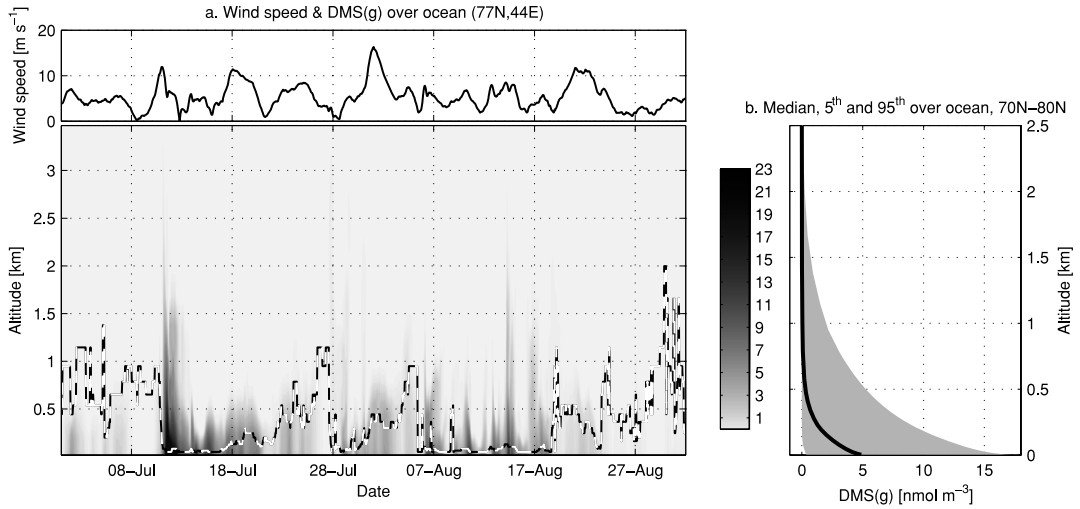

Fig. 2. (a) Low-level wind speed (m s^{-1}) and time-height cross section of DMS(g) (nmol m^{-3}) (grey shading) for a grid point over Barents Sea (77°N, 44°E) together with boundary layer height [km] (dashed line). (b) DMS(g) profiles over ocean from 70°N to 80°N, median profile (black line), 5th and 95th percentile (grey shaded area).

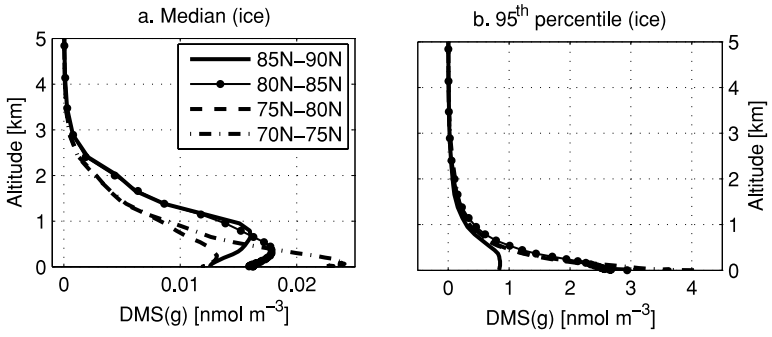

Fig. 3. (a) Median and (b) 95th DMS(g) profiles over ice for four 5-degree wide latitude bands from 70°N to 90°N. Latitude band 85°N–90°N (solid line), latitude band 80°N–85°N (line with dot), latitude band 75°N–80°N (dashed line) and latitude band 70–75N (dash–dotted line).

As can be seen in Fig. 3a the maximum median DMS(g) concentration is low relative to DMS(g) over open ocean, varying from 0.013 to 0.024 nmol m^{-3}. The modelled DMS(g) is biased towards lower values as there is no DMS(g) source over the pack-ice in the model (see Section 2.2). The height of the maxima increases northward from 150 m in latitude band 70°N–75°N (close to the DMS(g) source) to 750 m in latitude band 85°N–90°N (over the North Pole region). This is due to the combined effect of vertical mixing, increasing horizontal wind speeds with height and photo-chemical decay. When entering over the ice, the highest concentration is found near the surface and is distributed in a rather deep well-mixed boundary layer. The depth of the turbulent layer is shallower over the cold ice, thus the DMS(g) concentration above this layer is not any longer affected by turbulent mixing. The wind speed in this upper layer is stronger, thus at a certain distance from the ocean (approximately by the latitude bands) the travelling times are shorter (less photo-chemical decay) than close to the surface resulting in higher DMS(g) concentrations. Above the peak, DMS(g) concentration decreases exponentially and is close to zero at 4 km (Fig. 3a).

The 95th percentile DMS(g) profiles have significantly higher values and vary from 0.8 to 4.0 nmol m^{-3} at the surface (Fig. 3b). In latitude band 85°N–90°N (over the North Pole region), DMS(g) concentration increases from 0.8 nmol m^{-3} at the surface to 0.9 nmol m^{-3} at 200 m followed by an exponential decrease and is almost zero at 4 km. DMS(g) concentration in the remaining three profiles decreases exponentially above the surface and is close to zero at 4 km (Fig. 3b).

It is interesting to note that the median concentration of DMS(g) in the height interval 1.5–3 km over ice is higher than over the open ocean (not shown). Even if the concentrations at these heights are very low (<0.005 nmol m^{-3}) this indicates that other processes than turbulent mixing are responsible for bringing the DMS(g) to these altitudes.

Figure 4 shows time-height cross section of DMS(g) from a grid point over the pack-ice (85°N, 84°E) for July and August, 2001. The location is chosen for illustration of the vertical DMS(g) distributions that are found generally over the ice. DMS(g) advection occurs in plumes from the source region over the open ocean and in over the pack-ice area (Lundén et al., 2007). DMS(g) plumes are seen in Fig. 4 as episodes with increased concentration followed by periods when the surface concentration is close to zero. Note that the maximum concentration in the plumes at this location is higher in August than in July. The figure also shows occasions when DMS(g) concentrations are higher above the local boundary layer compared to the concentration at the surface, for example on July 16 and August 8. These maxima can be seen at different altitudes and with various temporal and vertical extent but more frequently when the boundary layer is less than 200 m deep. The maxima do not seem to have any connection to presence of modelled clouds. Such events are discussed further in the following sections.

3.3. Statistical inventory of DMS(g) maxima over ice

As discussed above, episodes over the pack-ice can be seen where DMS(g) concentration is significantly higher above the local boundary layer compared to the surface concentration (Fig. 4). These episodes are hereafter referred to as 'DMS(g) maxima.' To detect these episodes for a statistical inventory, three criteria are used to define a DMS(g) maximum and the sensitivity to these criteria are also examined. The Atlantic sector of the Arctic Ocean (see Section 2.2) is used as an example of the occurrence of DMS(g) maxima in the Arctic atmosphere. The criteria are:

(i) DMS(g) concentration should be 50% higher at a given altitude compared to the surface concentration at the same location.

(ii) Maximum DMS(g) concentration should be higher than 1 nmol m^{-3}.

(iii) The altitude at which the maximum occurs should be above the local boundary layer.

Figure 5 shows the median DMS(g) concentrations at all heights along with variability, represented by the 5th and 95th percentiles (grey shaded area). All profiles for the two simulated months over the pack-ice in the Atlantic sector that fulfill the criteria above are included. The figure shows a distinct peak of 1.3 nmol m^{-3} at approximately 350 m (5.1 nmol m^{-3} for the 95th percentile). Above this maximum, the median DMS(g)

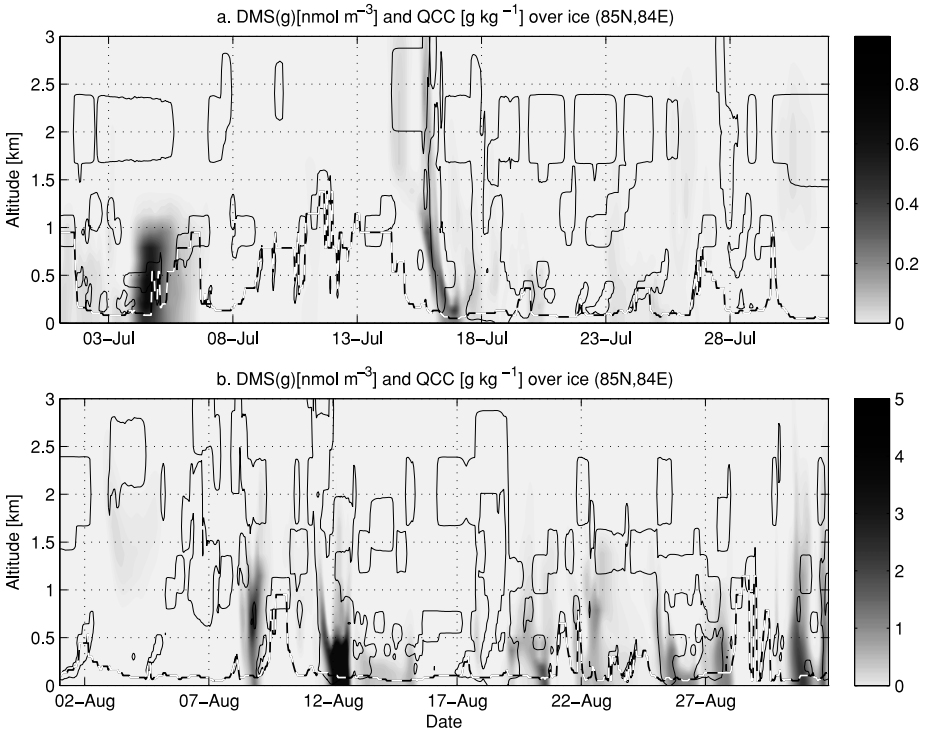

Fig. 4. Time-height cross section for (a) July and (b) August, 2001 for a grid point over ice (85°N, 84°E) of DMS(g) (nmol m^{-3}) (grey shading), black line indicates cloud water content of 0.01 g kg^{-1} and boundary layer depth (km) (dashed line). Note the difference in scale in (a) and (b).

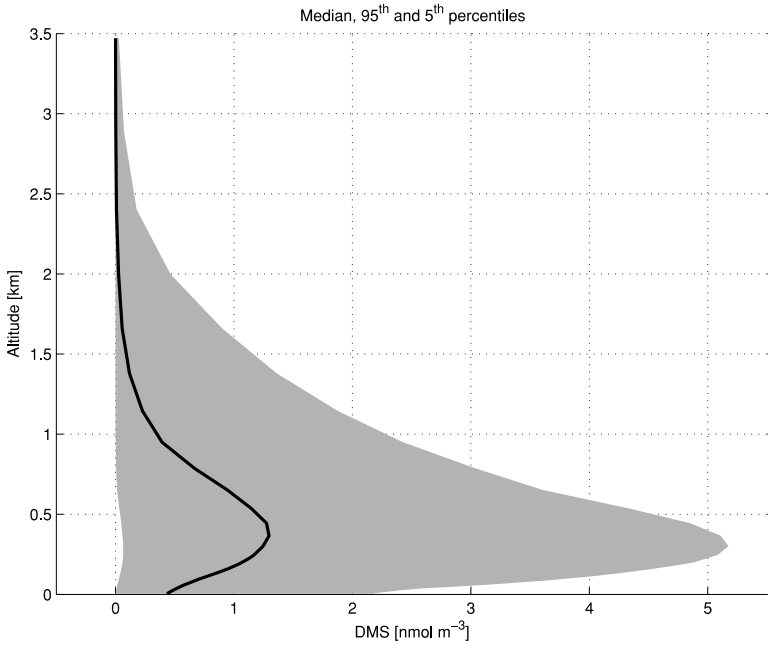

Fig. 5. Median (black line), 5th and 95th percentiles (grey shaded area) for DMS(g) concentrations at model height over ice in the Atlantic sector of the Arctic Ocean (70°N–90°N, 70°W–90°E) using the 50% and 1 nmol m^{-3} criteria, for July and August 2001.

concentrations decrease almost linearly with altitude to about 1 km height and then exponentially approaches zero at 2 km (2.5 km for the 95th percentile). In this example, 5% of the DMS(g) profiles over ice in the Atlantic sector fulfil the criteria defined above. This is significantly higher compared to the frequency of DMS(g) maxima found over open ocean which is 0.5% in this sector of the Arctic Ocean.

A sensitivity study shows that changing criteria 2, from 1 to 0.5 nmol m^{-3} or 0.1 nmol m^{-3}, increases the number of DMS(g) maxima over ice to 8 or 15%, respectively. Similarly, changing

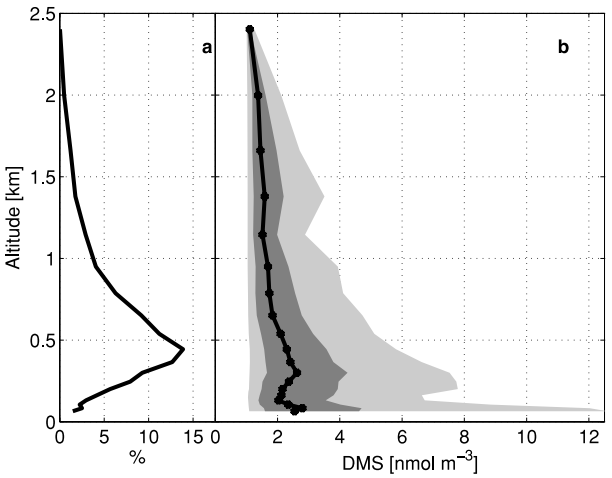

Fig. 6. Occurrence and height of DMS(g) maxima in profiles from the Atlantic sector of the Arctic Ocean for July and August 2001 that fulfil the 50% and 1 nmol m^{-3} criteria. Shown are (a) the percentage of occurrence of maxima found at each height, and, (b) median maxima concentrations (black line), 5th and 95th percentiles (light grey shaded area), 25th and 75th percentiles (dark grey shaded area).

criteria 1 from 50 to 30% increases the number of DMS(g) maxima over ice to 7% (1 nmol m^{-3}) or 19% (0.1 nmol m^{-3}). When applying the original criteria on DMS(g) profiles over the whole ice covered region about 3% of the profiles covering both time and space have an elevated maximum. There are no significant variations with distance from ice-edge. When the analysis is performed in the four latitude bands discussed in Section 3.2, approximately 3% of the DMS(g) profiles fulfil the criteria (50% and 1 nmol m^{-3}).

Figure 6 presents the results of an analysis of each profile that fulfil the criteria for the Atlantic sector. Presented in the figure are the median and percentiles (5th, 25th, 75th and 95th) for the maximum concentrations and their respective heights Fig. 6b. The maximum concentrations are preferably found at certain specific heights, 85, 300 and 1400 m, above the surface. The maximum at 100 m is not far above the local boundary layer and have the highest median (and percentile) concentrations. However, there are very few cases, only 2–3% of all maxima are found at this height. Most frequently, maxima are found between 200 and 700 m height (Fig. 6a), about 70% of the maxima are found in this interval. The median maxima in this layer is just above 2 nmol m^{-3} but 25% of the data has maxima higher than about 4 nmol m^{-3} (Fig. 6a). It is interesting to note that in about 2% of the cases, the maxima is located at 1.4 km height with concentrations in the range 1.0–3.5 nmol m^{-3} (5th and 95th percentiles).

3.4. Profile observations of DMS(g)

The statistical inventory indicates that modelled DMS(g) maxima occur in the Arctic atmosphere over the pack-ice region. Measurements of DMS(g) concentration are scarce in the Arctic relative to lower latitudes and specially concerning the vertical distribution of DMS(g) where only a few observations are available. During the Arctic Ocean Expedition 2001 (AOE-2001, Leck et al., 2004; Tjernström et al., 2004), 36 helicopter flights were carried out over the pack-ice region and during 14 of them DMS(g) measurements were made with a Proton Transfer Reaction Mass Spectrometer System (PTR-MS, Lindinger et al., 1998). Most of them, however, show concentrations below the detection limit of the instrument; a variable interference noise estimated to be about 1 nmol m^{-3}. Figure 7 shows observations taken during two flights on August 24, between 19:00–20:00 UTC and 22:00–23:00 UTC. The flights were made north of Svalbard (83°N, 17°E) in the marginal ice zone, thus, the observations are taken over ice and some open water. The observations presented at 27 m a.s.l in Fig. 7 are from a second PTR-MS instrument on-board the icebreaker.

At the time of the observations, both the observed and modelled temperature structures display strong surface inversions

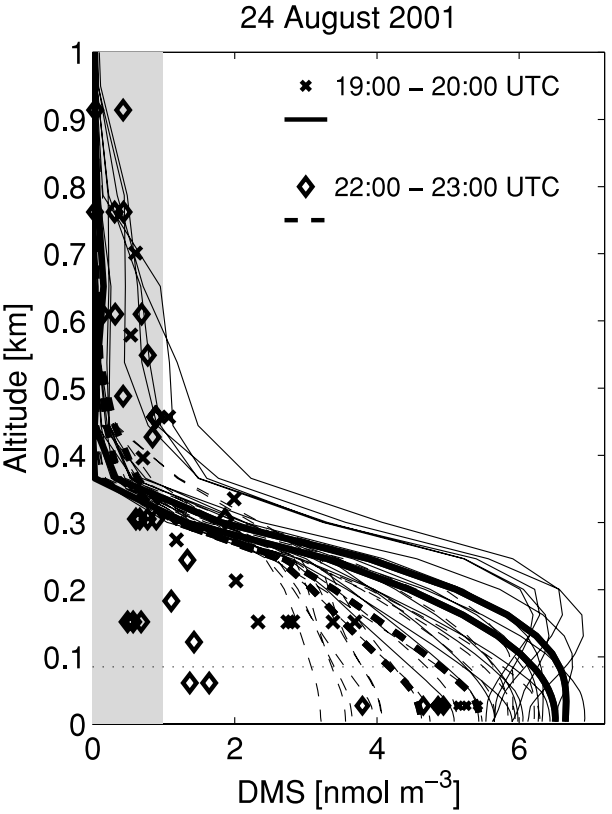

Fig. 7. Observed (markers) and modelled (lines) DMS(g) (nmol m^{-3}) at (83°N, 17°E) for August 24, 2001 at 19:00–20:00 UTC (crosses and solid lines) and 22:00–23:00 UTC (diamonds and dashed lines). The model column corresponding to the time and location of the observations (thick lines) as well as the surrounding locations (thin lines) are also shown in the figure. The shaded area shows an estimate of the detection limit for the instrument.

(not shown) and the model diagnosed a boundary layer depth of 85 m. The profiles show a history of a about 400 m deep boundary layer over the ocean before being advected in over the pack ice while experiencing significant cooling at the surface resulting in the stably stratified atmosphere from the surface and up. In Fig. 7, DMS(g) concentrations from the grid column and times corresponding to the observations are shown together with the observations and it is clear that the air mass recently has been over the ocean where the DMS(g) were mixed up to about 400 m a.s.l. The model simulation is performed using a large domain (see Fig. 1), thus perfect agreement in time and space between the model and observations is not expected. The model is not constrained enough by the boundary conditions; the synoptic scale evolution may diverge from the observed one. Thus, in addition to the corresponding modelled profiles, results from the surrounding eight grid columns are also shown representing an area of 150×150 km^2.

The model profiles show significant concentrations of DMS(g) in a layer from the surface and up to 450 m a.s.l. at the time of the observations. When considering the larger area, the model show concentrations above zero up to altitudes of 1 km. This is in agreement with the observations that show concentrations well above the detection limit up to about 450 m and indicate concentrations above zero up to about 1 km. Thus, DMS(g) is present above the local boundary layer in both model and observations. Concentrations up to 4 nmol m^{-3} are observed during the earlier helicopter flight in the layer 150–350 m a.s.l. The modelled concentrations of DMS(g) are higher at these altitudes but the structure of both profiles are similar to the ones found over the open ocean (see Fig. 2b). Both observed and modelled concentrations of DMS(g) are lower at the time of the second flight. At this time, the observed concentrations from the ship-based observations are quite different from the ones observed from the helicopter. The data below 15 m comes from a flight leg over a large lead southwest of the ice breaker. This could possibly indicate that the local DMS flux here is downward (Leck and Persson, 1996a), thus reducing the near-surface concentration; a small-scale process not resolved in the model. Other aircraft measurements of DMS(g) at multiple altitudes have been reported from the Arctic atmosphere by Ferek et al. (1995). They measured DMS(g) concentrations of 0.2, 0.3 nmol m^{-3} at 1527 m; 1.3, 2.5 and 4.8 nmol m^{-3} at 1374 m; and 0.4 nmol m^{-3} at 1069 m. These observations were obtained over both ice and open water, near Barrow (71°N, 152°W) in June 1990. More recently profile observations of DMS in the high Arctic were performed during the Arctic Summer Cloud Ocean Study (ASCOS, www.ascos.se). During this ice-breaker expedition to the high Arctic during summer 2008, in total eight helicopter flights with DMS observations were performed; seven north of 87°N and one in the marginal ice zone at 82.4°N. All profiles over the ice show as high or higher concentrations, compared with near-surface values, at altitudes 500–1000 m a.s.l. which in all cases is above the local boundary layer (personal communication, Martin Graus). These observed profiles shape do indeed resemble the ones found in the model (Fig. 3). The profile taken in the marginal ice zone area shows high concentrations, much higher than further north, in a layer from the surface and up to 200 m consistent with being so close to the source area. A secondary maximum at 700 m a.s.l. is also observed.

The above discussed observations support the model results and the conclusion that significant DMS(g) concentrations do exist in the Arctic atmosphere at altitudes not to be expected when only considering vertical mixing in the boundary layer.

3.5. *The formation and fate of DMS(g) maximum*

The advantage of using a 3-D model on a regional scale is the possibility to include both the pack-ice area and DMS source regions in the open oceans in a three dimensional dynamically constrained picture. This is in particular helpful for the understanding of the formation of DMS(g) maxima.

Consider as an example the maximum at August 28, 2001 (Fig. 4b). Figure 8a shows the synoptical situation at this time. A high pressure center ($>$1022 hPa) is located over Barents Sea. Low pressure centers ($<$1000 hPa) are located over the central parts of the pack-ice and over the Greenland Sea (Fig. 8a). The flow is anticlockwise around the low pressure centre over the pack-ice, advecting DMS(g) from the Barents, Greenland and Kara Sea region in over the pack-ice in a well-defined plume (Fig. 8b). The concentration in the plume is gradually decreasing during the advection in over the ice starting from a concentration of about 5 nmol m^{-3} close to the source. Fig. 8c shows the horizontal distribution of DMS(g) at 538 m, i.e. the height of the elevated maximum (see Fig. 4a). The plume extends approximately 280 km in over the pack-ice, following the flow around the low pressure, reaching further in over the ice at this height compared to closer to the surface (Fig. 8b).

Figures 8d–f show the vertical cross section, from the surface up to 2.5 km, of equivalent potential temperature (θ_e)[1], DMS(g), cloud water content and turbulent kinetic energy along the line of grid points indicated by a thick line in Figs. 8a–c. A sector of cold air with equivalent potential temperatures <2 °C in the boundary layer is located between grid points 60 and 66. This layer is turbulent and cloud topped (Fig. 8e). A frontal zone is evident between this cold air and a sector of warm air, found east of grid point 66. This air mass is stably stratified and the shear-produced turbulence near the surface is not connected to the turbulent cloud layer. The warm air mass contains high concentrations of DMS(g) >2 nmol m^{-3} at 500 m a.s.l. which is clearly above the local boundary layer. This maximum is present due to the general lifting of the warm air mass while advected in over the pack-ice. In this case the vertical distribution of DMS(g) is thus

[1] $\theta_e = \theta + \frac{L\theta}{C_p T} q$, where θ is the mean potential temperature, q is the specific water vapor and T is the mean temperature at the lifting condensation level.

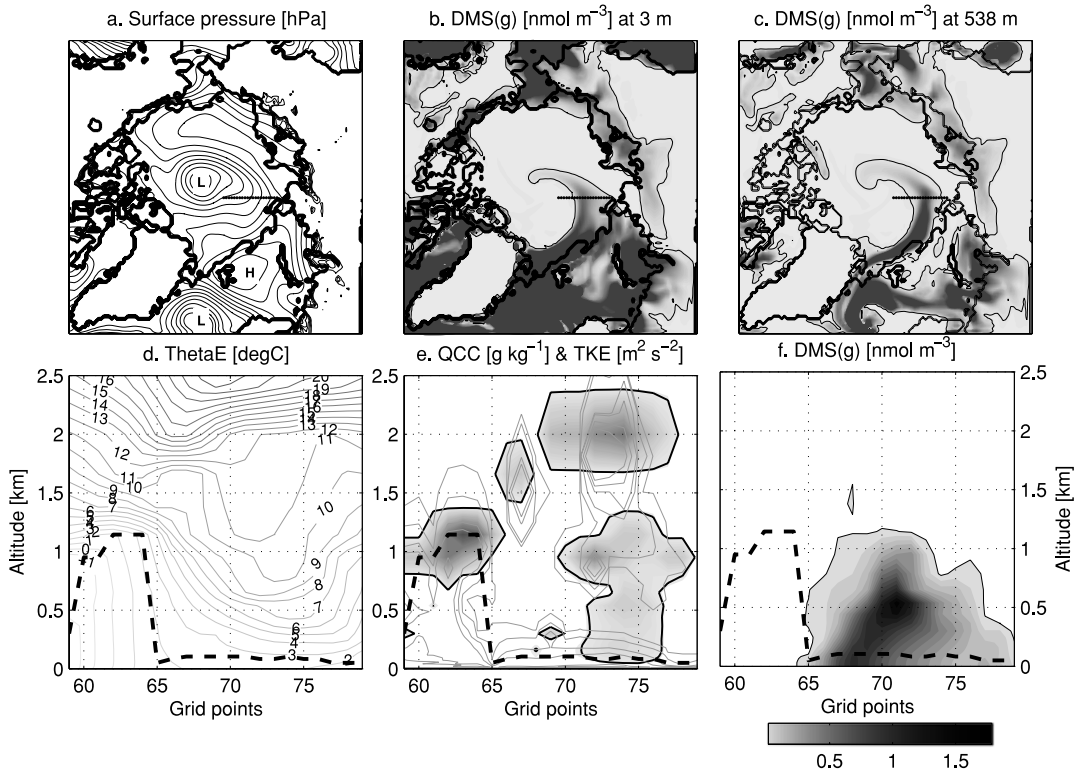

Fig. 8. (a) Surface pressure (hPa), (b) horizontal distribution of DMS(g) (nmol m^{-3}) at 3 m and (c) at 538 m for August 28, 2001. Vertical distribution of (d) equivalent potential temperature (°C), (e) cloud water content, black line indicates cloud water content of 0.01 g kg^{-1} and turbulent kinetic energy of 0.001, 0.01, 0.05, 0.1, 0.3 and 0.5 m^2 s^{-2} as grey contour lines and (f) DMS(g) (nmol m^{-3}), for 10 grid points indicated in the panels in the upper row. Boundary layer depth (km) as dashed lines. Black contour line in panel b, c and f indicates DMS(g) concentration of 0.1 nmol m^{-3}.

formed in connection to a frontal zone. The fate of this maximum is investigated further by examining the time evolution in grid point 69.

Figure 9 shows time-height cross sections at grid point 69 (see Figs. 8d–f) of equivalent potential temperature, DMS(g), wind speed, cloud water content and turbulent kinetic energy for August 27–30, 2001. At the beginning of the period, August 27, the cold air mass is being replaced with the warm DMS(g)-containing air. In the warm air mass, there is a low-level jet at 200 m a.s.l. (Fig. 9c). The shear below the jet creates turbulence and vertical mixing, thus the DMS(g) is transported downwards and the near-surface concentration is increasing (Fig. 9b). This extra source of DMS(g) from aloft and its oxidation products may hence influence the growth to CCN and aid cloud formation within the boundary layer. The near-surface concentration drops quickly when the warm air is replaced with a cold air mass on August 29.

4. Summary

This model study focus on the vertical distribution of DMS(g) in the Arctic region (north of 70°N). The atmospheric part of COAMPS® was used to simulate DMS(g) concentration over the pan-Arctic during the summer season, July and August 2001.

The results show that median DMS(g) concentration over ocean is highly influenced by its source, with highest DMS(g) concentrations close to the surface and declined exponentially with altitude and are close to zero at 2 km. Over the pack-ice, episodes when DMS(g) concentration are higher above the local boundary layer relative to the surface concentration are found. These DMS(g) maxima are defined as profiles with a DMS(g) maximum concentration of at least 1 nmol m^{-3} and with 50% higher concentration above the local boundary layer compared to the near-surface concentration. A statistical inventory over the pack-ice in the Atlantic sector of the Arctic Ocean (70°N–90°N, 70°W–90°E) show that such DMS(g) maxima are present in about 5% of all the model profiles. As a comparison, DMS(g) maxima are present in 0.5% of the vertical profiles over ocean in the same sector. The results also show that there is no typical DMS(g) maximum. These maxima occur at different altitudes (above the local boundary layer), and with various temporal and vertical extents. In about 70% of the cases, the maximum concentrations are found at heights between 200 and 700 m a.s.l.

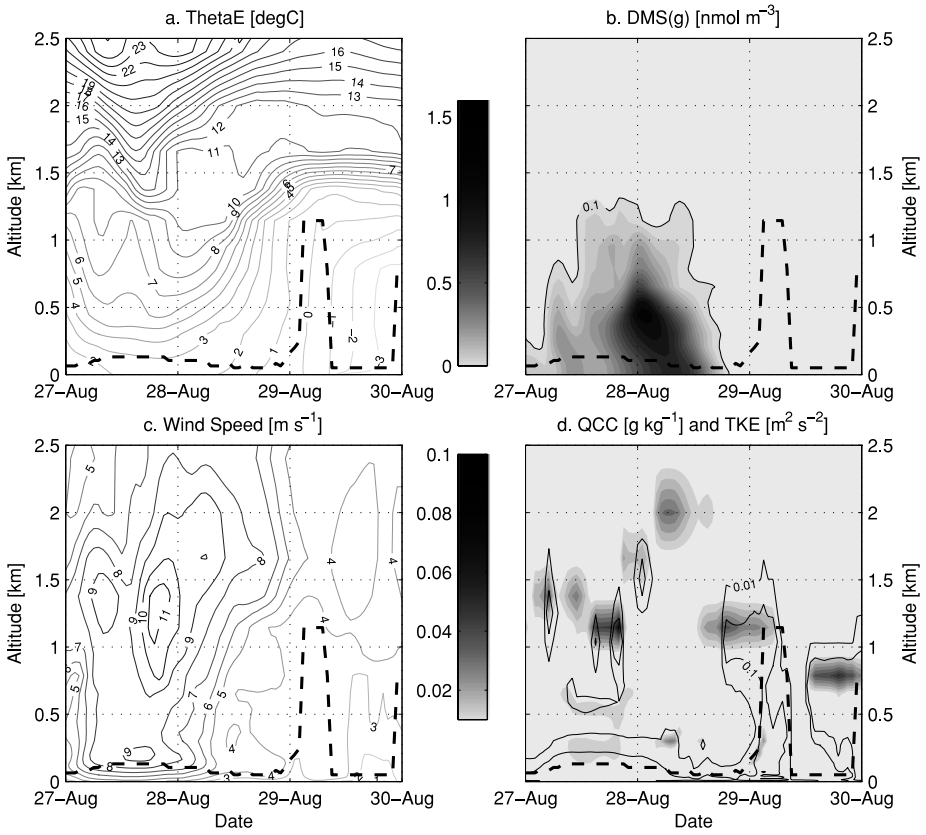

Fig. 9. Time-height cross section of (a) equivalent potential temperature (°C), (b) DMS(g) (nmol m^{-3}), (c) wind speed (m s^{-1}), (d) cloud water content (g kg^{-1}) (grey shading) and turbulent kinetic energy of 0.1 m^2 s^{-2} and 0.01 m^2 s^{-2} (black contour lines) for August 27–31, 2001. Boundary layer depth (km) as dashed lines.

Observations in the high Arctic of DMS(g) above the surface are extremely rare. Here we present data from two helicopter flights, from August 24, 2001 at (83°N, 17°E). These flights were the only two, out of 14 flights, that showed concentrations significantly above the detection limit of the PTR-MS instrument. Both the observations and the model profiles show significant concentrations well above the shallow local boundary layer at this location.

Bigg et al. (1996, 2001) observed unexpected rapid changes in DMS(g) near-surface concentration over the pack-ice area and speculated that these changes could be associated with downward mixing of DMS(g) in connection to frontal zones. Leck and Persson (1996b) demonstrated in a case study that sudden increases of DMS(g) over the pack-ice region could be due to downward mixing from a larger source aloft in association to the passage of a warm front.

Our model results show that DMS(g) maxima can be found in connection to a frontal zone. The DMS(g) is transported from the source area over the open ocean in a warm air mass that glides on top of a cold air mass and end up above the local boundary layer in over the pack-ice area. Occasionally, in the presence of turbulence, DMS(g) can then be mixed down and act as a local source of DMS oxidation products contributing to cloud formation in the boundary layer.

5. Acknowledgments

We thank Laurent Brodeau and Stefan Söderberg for assistance with COAMPS®, Matthias Karl for calculating the decay rate of atmospheric DMS and Martin Graus and Markus Müller for experimental data. We gratefully acknowledge financial support from the Stockholm University, the Austrian BMWF, and the Leopold-Franzens University of Innsbruck. We gratefully acknowledge the Naval Research Laboratory for making COAMPS® available, the European Centre for Medium-Range Weather Forecast for providing the re-analysis fields and the National Supercomputer Centre in Sweden for computer resources.

References

Atkinson, R., Baulch, D. L., Cox, R. A., Crowley, J. N., Hampson, R. F. J. and co-authors. 2004. Summary of evaluated kinetic and photochemical data for atmospheric chemistry; IUPAC subcommittee

on gas kinetic data evaluation for atmospheric chemistry, http://www.iupac-kinetic.ch.cam.ac.uk/.

Bates, T. S., Cline, J. D., Gammon, R. H. and Kelly-Hansen, S. R. 1987. Regional and seasonal variations in the flux of oceanic dimethylsulfide to the atmosphere. *J. Geophys. Res.* **92**(C3), 2930–2938.

Bigg, E. K., Leck, C. and Nilsson, E. D. 1996. Sudden changes in the Arctic atmospheric aerosol concentration during summer and autumn. *Tellus* **48B**, 254–271.

Bigg, K. C., Leck, C. and Nilsson, E. D. 2001. Sudden changes in aerosol and gas concentrations in the central Arctic marine boundary layer: causes and consequences. *J. Geophys. Res.* **106**(D23), 32 167–32 185.

Birch, C. E., Brooks, I. M., Tjernström, M., Milton, S. F., Earnshaw, P. and co-authors. 2009. The performance of a global and mesoscale model over the central Arctic ocean during late summer. *J. Geophys. Res.* **114,** D13104, doi:10.1029/2008JD010790.

Bouillon, J.-C., Lee, P., de Mora, S., Levasseur, M. and Lovejoy, C. 2002. Vernal distribution of dimethylsulphide, dimethylsulfoniopropionate and dimethylsulphoxide in the North Water Polynia, northern Baffin Bay, in 1998. *Deep-Sea Res.* **Part II 49**, 5171–5189.

Capaldo, K. P. and Pandis, S. N. 1997. Dimethyl sulfide chemistry in the remote marine atmosphere: evaluation and sensitivity analysis of available mechanisms. *J. Geophys. Res.* **102**(D19), 23 251–23 267.

Charlson, R. J., Lovelock, J. E., Andreae, M. O. and Warren, S. G. 1987. Oceanic phytoplankton, atmospheric sulfur, cloud albedo and climate. *Nature* **326**, 655–661.

Curry, J. A. 1995. Interactions amoung aerosols, cloud and climate of the Arctic Ocean.. *Sci. Tot. Env.* **160/161**, 777–791.

Ferek, R. J., Hobbs, P. V., Radke, L. F., Herring, J. A., Sturges, W. T. and co-authors. 1995. Dimethyl sulfide in the Arctic atmosphere. *J. Geophys Res.* **100**(D12), 26 093–26 104.

Heintzenberg, J. and Leck, C. 1994. Seasonal variation of the atmospheric aerosol near the top of the marine boundary layer over Spitzbergen related to the Arctic sulphur cycle. *Tellus* **46**(B), 52–67.

Hodur, R. M. 1997. The Naval Research Laboratory's Coupled Ocean-Atmosphere Mesoscale Prediction System (COAMPS). *Mon. Wea. Rev.* **125**, 1414–1430.

Intrieri, J. M., Shupe, M. D., Uttal, T. and McCarty, B. J. 2002. An annual cycle of Arctic cloud characteristics observed by radar and lidar at SHEBA. *J. Geophys. Res.* **107**(C10), 5:1–17.

Karlsson, J. and Svensson, G. 2010. The simulation of Arctic clouds and their influence on winter surface temperature in present day climate in the CMIP3 multi-dataset. *Clim. Dyn.,* doi:10.1007/s00382-010-0758-6.

Kettle, A. J., Andreae, M. O., Amouroux, D., Andreae, T. W., Bates, T. S. and co-authors. 1999. A global database of sea surface dimethylsulfide (DMS) measurements and a procedure to predict sea surface DMS as a function of latitude, longitude, and month. *Global Biogeochem. Cycles* **13**, 399–444.

Klein, S. A., McCoy, R. B., Morrison, H., Ackerman, A. S., Avramov, A. and co-authors. 2009. Intercomparison of model simulations of mixed-phase clouds observed during the ARM Mixed-Phase Arctic Cloud Experiment. I: single-layer cloud. *Quart. J.* **135**, 979–1002.

Leck, C. and Bigg, E. K. 2005. Source and evolution of the marine aerosol—a new perspective. *Geophys. Res. Lett.* **32**, 1–4.

Leck, C. and Bigg, E. K. 2007. A modified aerosol-cloud-climate feedback hypothesis. *Environ. Chem.* **4**, 400–403.

Leck, C., Bigg, K. E., Covert, D. S., Heintzenberg, J., Maenhaut, W. and co-authors. 1996. Overview of the atmospheric research program during the International Arctic Ocean Expedition of 1991 (IAOE-91) and its scientific results. *Tellus* **48B**, 136–155.

Leck, C. and Persson, C. 1996a. The central Arctic Ocean as a source of dimethyl sulfide—seasonal variability in relation to biological activity. *Tellus* **48B**, 156–177.

Leck, C. and Persson, C. 1996b. Seasonal and short-term variability in dimethyl sulfide, sulfur oxide and biogenic sulfur and sea salt aerosol particles in the Arctic marine boundary layer during summer and autumn. *Tellus* **48B**, 272–299.

Leck, C., Tjernström, M., Matrai, P., Swietlicki, E. and Bigg, E. K. 2004. Can marine micro-organisms influence melting of the Arctic pack ice?. *EOS Trans. Am. Geophys. Un.* **85**(3), 25,30,32.

Levasseur, M., Gosselin, M. and Michaud, S. 1994. A new source of dimethylsulfide (DMS) for the Arctic atmosphere-ice diatoms. *Mar. Biol.* **121**, 381–387.

Lindinger, W., Hansel, A. and Jordan, A. 1998. Proton-transfer-reaction mass spectrometry (PTR-MS): on-line monitoring of volatile organic compounds at ppt levels. *Chem. Soc. Rev.* **27**, 347–354.

Liss, P. and Merlivat, L. 1986. Air-sea gas exchange rates: introduction and synthesis: the role of air-sea exchange in geochemical cycling Liss, P. and Merlivat, L. D. Reidel Publishing Co. Edit by P. Buat-Meénard.

Lohmann, U. and Leck, C. 2005. Importance of submicron surface-active organic aerosols for pristine Arctic cloud. *Tellus* **57B**, 261–268.

Lundén, J., Svensson, G. and Leck, C. 2007. Influence of meteorological processes on the spatial and temporal variability of atmospheric dimethyl sulfide in the high Arctic summer. *J. Geophys. Res.* **112**(D13).

Matrai, P. A. and Vernet, M. 1997. Dynamics of the vernal bloom in the marginal ice zone of the Barents Sea: dimethyl sulfide and dimethylsulfoniopropionate budgets. *J. Geophys Res.* **102**(C10), 22 965–22 979.

Rinke, A., Dethloff, K., Cassano, J., Christensen, J. H., Curry, J. A. and co-authors. 2006. Evaluation of an ensemble of Arctic regional climate models: spatial patterns and height profiles.. *Clim. Dyn.* **26**, 459–472.

Sharma, S., Barrie, L. A., Plummer, D., McConnell, J. C., Levasseur, P. C. B. M. and co-authors. 1999. Flux estimation of oceanic dimethyl sulfide around North America. *J. Geophys. Res.* **104**(D17), 21 327–21 342.

Staubes, R. and Georgii, H.-W. 1993. *Dimethylsulfide: Oceans, Atmosphere, and Climate: Measurements of Atmospheric and Seawater DMS Concentrations in the Atlantic, Arctic and Antarctic Region*. (eds G. Restelli and G. Angeletti), Kluwer Academic Publishers, Brussels and Luxembourg.

Stockwell, W. R., Kirchner, F., Kuhn, M. and Seefeld, S. 1997. A new mechanism for regional atmospheric chemistry modeling. *J. Geophys. Res.* **102**, 25 847–25 879.

Tjernström, M. 2005. The summer Arctic boundary layer during the Arctic Ocean Experiment 2001 (AOE-2001). *Bound.-Layer Meteorol.* **117**(1), 5–36.

Tjernström, M., Leck, C., Persson, P. O. G., Jensen, M. L., Oncley, S. P. and co-authors. 2004. The summertime Arctic atmosphere: meteorological measurements during the Arctic Ocean Experiment 2001 (AOE-2001). *Bull. Am. Met. Soc.* **85**, 1305–1321.

Tjernström, M., Sedlar, J. and Shupe, M. D. 2008. How well do regional climate models reproduce radiation and clouds in the Arctic? An evaluation of ARCMIP simulations. *J. Appl. Meteorol. Climatol.* **47**, 2405–2422.

Tjernström, M., Zagar, M., Svensson, G., Cassano, J., Pfeifer, S. and co-authors. 2005. Modelling the Arctic boundary layer: an evaluation of six ARCMIP regional-scale models with data from the SHEBA project. *Bound.-Layer Meteorol.* **117**(2), 337–381.

Wyser, K., Jones, C. G., Du, P., Girard, E., Willén, U. and co-authors. 2008. An evaluation of Arctic cloud and radiation processes during the SHEBA year: simulation results from eight Arctic regional climate models. *Clim. Dyn.* **30**, 203–223.